Polymer Degradation and Stability 177 (2020) 109192

Contents lists available at ScienceDirect

Polymer Degradation and Stability

journal homepage: www.elsevier.com/locate/polydegstab

Effects of pure and intercalated halloysites on thermal properties of phthalonitrile resin nanocomposites

Shengnan Bai [a], Xinyu Sun [a], Minjie Wu [a], Xiaoyu Shi [a], Xinggang Chen [b], Xiaoyan Yu [a, *], Qingxin Zhang [a, c, **]

[a] Hebei Key Laboratory of Functional Polymers, School of Chemical Engineering and Technology, Hebei University of Technology, Tianjin, 300130, China
[b] School of Materials Science and Engineering, North China University of Science and Technology, Tangshan, 063210, China
[c] Tianjin Key Laboratory of Materials Laminating Fabrication and Interface Control Technology, Hebei University of Technology, Tianjin, 300130, China

ARTICLE INFO

Article history:
Received 9 March 2020
Received in revised form
10 April 2020
Accepted 11 April 2020
Available online 19 April 2020

Keywords:
Phthalonitrile resin
Halloysite nanotubes
Nanocomposites
Thermomechanical properties
Thermal stability

ABSTRACT

In this work, composite materials with different halloysite nanotubes (HNTs) content as fillers were prepared by using phthalonitrile resin with alkyl center as matrix. In order to improve the dispersibility of HNTs in the polymers, phenylphosphonic acid (PPA) was used to treat HNTs. The results of Wide-angle X-ray Diffraction (WAXD), Fourier Transform Infrared spectroscopy (FTIR), Thermogravimetric Analysis (TGA) and Scanning Electron Microscope (SEM) showed that when the mass ratio of PPA to HNTs was 2:1, the intercalation rate of HNTs was the highest. The thermomechanical properties, thermal stability and thermal oxidation stability of the composite were tested by Dynamic Mechanical Analysis (DMA) and Thermogravimetric analysis (TGA). The results indicated that the polymers with intercalated HNTs as fillers have better thermomechanical properties than those with pure HNTs as fillers. When the modified HNTs content was 7%, the storage modulus of the polymer increased by 16.52% and 15.43% at 30 °C and 380 °C, respectively. With the increase of fillers, the thermal stability of polymers with pure HNTs as fillers increased, while that of polymers with modified HNTs as fillers increased first and then decreased. On the other hand, the limit oxygen index (LOI) of the polymers also increased to some extent. The degradation and control of the nanocomposites at high temperature were discussed. SEM was used to observe the cross-section morphology and found that pure HNTs would agglomerate in the polymer. The thermal properties of the phthalonitrile resin were improved by using the wide source HNTs as fillers.

1. Introduction

With the continuous development of the society, polymer materials play an increasingly important role. Phthalonitrile resins are high performance thermosets with superior flame resistance, excellent thermomechanical properties and outstanding stability at high temperature [1–4]. These advantages will make them show great application prospects in such fields as aerospace, electronic packaging, etc [5–7]. In order to further improve the properties of phthalonitrile resin and expand its application fields, many researchers have done lots of research on phthalonitrile resin composites. Liu et al. prepared phthalonitrile resin with excellent thermal conductivity using boron nitride as the filler, and the resin showed excellent thermal stability and thermomechanical properties [8]. At the same time, some novel nanoparticles such as Al_2O_3-water nanofluid [9], cadmium sulfide [10], nanocellulosic fiber [11], sisal nanofibril [12], F-doped $TixV_{1-x}O_2$ [13], electrospun polyimide (PI) nanofibers [14] and nanostructured CuO thin films [15] have been developed. In addition, some common inorganic fillers such as alumina [16], zinc oxide [17], titania [18], silicon nitride [19] and graphene [20] have also been successfully used in the preparation of phthalonitrile resin composites. Most of the inorganic fillers mentioned above are nanoparticles. So researchers use silane coupling agent or other substances to modify the surface of fillers to improve the dispersion of inorganic particles in polymers. After the fillers were added, the phthalonitrile resins show better performance than the pure resins.

* Corresponding author.
** Corresponding author. Hebei Key Laboratory of Functional Polymers, School of Chemical Engineering and Technology, Hebei University of Technology, Tianjin, 300130, China.
E-mail addresses: yuxycnn@163.com (X. Yu), zhqxcn@163.com (Q. Zhang).

https://doi.org/10.1016/j.polymdegradstab.2020.109192
0141-3910/

Among many inorganic fillers, halloysite nanotubes (HNTs) have attracted the attention of researchers due to their wide source, low price and excellent thermal stability [21–23]. The main component of halloysite is aluminosilicate with hollow tubular structure whose chemical formula is $Al_2Si_2O_5(OH)_4 \cdot 2H_2O$ [24,25]. Du et al. prepared a composite of polypropylene and HNTs by melt blending. The results showed that the addition of HNTs significantly improved the thermal stability of the matrix. And it is proposed that the improvement of thermal stability is due to the mechanism that HNTs can embed decomposition products [26]. For polymers, necessary instrumental test is very important. Dynamic mechanical analysis (DMA) is an excellent method to measure their storage modulus and glass transition temperature [27]. James et al. prepared a series of interpenetrating polymer networks (IPN) based on SBR and PMMA. They used DMA to analyze the degree of entanglement of polymer chains and connected them with morphology. The morphology was in good agreement with the theoretical prediction of DMA results [28]. At the same time, some polymer synthesis methods, such as click chemistry [29] and self-assembly [30], also play a huge advantage in the development of polymer field.

Because of the excellent properties of halloysite nanotubes, many researchers regard them as fillers of poly (ε-caprolactone) [31], epoxy resin [32,33], polylactic acid [34] and other materials. However, it is rarely reported as phthalonitrile resins filler. Aiming at improving the thermal properties of phthalonitrile resin, we used HNTs as the fillers to prepare the composite materials. Nanoparticles are easy to agglomerate. In order to improve the dispersion of HNTs in the matrix, phenylphosphonic acid (PPA) was used to modify them, and the optimal modification conditions were explored by changing the amount of PPA. The structure and properties of the HNTs and composite material were extensively studied by WAXD, FTIR, SEM, TGA and DMA. At the same time, the effect of HNTs on the degradation of polymers at high temperature was discussed. Due to the great properties of HNTs, the nanocomposites have more excellent thermal mechanical properties, thermal stability, thermal oxidation stability and are expected to be used in areas of aerospace, engine shell, electronic package and other fields.

2. Experimental section

2.1. Materials

Phenylphosphonic acid (PPA, AR,98%) was supplied by Shanghai Dibai Chemical Co.. Halloysite nanotubes (HNTs) was purchased from Guangzhou Yuanxin Nano Technology Co., and dried for 24 h at 60 °C. 4,4′,4″-Trihydroxytriphenylmethane (AR,98%) was supplied by Shanghai Bide Pharmaceutical Co.. 4-Nitrophthalonitrile (AR,98%) was purchased from Zhengzhou Alfa Chemical Co.. *N,N*-dimethylformamide (DMF, 99.5%) was purchased from Tianjin Hengshan Chemical Co.. Toluene was purchased from Tianjin Fuchen Chemical Co.. Anhydrous potassium carbonate (K_2CO_3, 99.0%) was purchased from Tianjin Hengshan Chemical Co., and dried for 24 h at 100 °C. All the solvents were used without further purification.

2.2. Chemical treatment of HNTs

HNTs (2g), PPA (1g, 6.33 mmol) and deionized water (100 mL) were added to a three-necked flask successively and the PPA was fully dissolved in water by stirring. Then, the mixture in the three-necked flask was vacuumed three times to make the inner part of halloysite nanotubes completely contact with PPA. Condenser tube was then connected to the three-necked flask and the mixture was stirred at 100 °C for 100 h. After the reaction, the mixture was filtered and washed with a large amount of deionized water to give the white filter cake. Finally, the collected products were vacuum dried at 60 °C for 24 h and marked as HNTs-a.

The modified HNTs samples of HNTs-b, HNTs-c and HNTs-d were prepared according to the method described above, except that the weight of PPA used for treatment was 2g, 4g and 6g, respectively. The chemical treatment of HNTs is shown in Scheme 1 [32,35].

2.3. Synthesis of 4-(aminophenoxy)phthalonitrile (APPH) monomer

APPH is a self-catalyzed benzonitrile monomer and was used as the curing agent, which was synthesized according to the procedures described in previously reported paper [36].

2.4. Synthesis of 4,4′,4"- [(methanetriyltris (benzene-4,1-diyl)) tris (oxy)] triphthalonitrile (MDTP) monomer

MDTP is a benzonitrile monomer with a low melting point and low viscosity, which was prepared in our laboratory by nucleophilic substitution reaction [37].

2.5. Preparation of HNTs–phthalonitrile resin nanocomposites

The first step was to fully mix HNTs and benzonitrile monomers in deionized water. HNTs-c (with the best modification effect) or pure HNTs were added into 1000 mL of deionized water according to 0%, 1%, 3%, 5%, and 7% of the weight of MDTP monomers. APPH was added into above mixed solution with 10% of the weight of MDTP monomers. Then the solution was respectively placed in magnetic stirring and ultrasonic environment for 3 h to ensure that the benzonitrile monomer and halloysite nanotubes were fully mixed. The mixture was then filtered and vacuum dried at 60 °C for 24 h. The second step was to make the mixture into polymers. The mixture was then placed in a pre-determined mold in a vacuum drying oven at 200 °C, and degassed in vacuum for about 20 min until the viscosity of the mixture was high and there was no large amount of bubbles. Finally, the mixture was rapidly transferred to the muffle furnace. The heating procedure of muffle furnace was as follows: 200 °C/2h, 230 °C/2h, 260 °C/4h, 290 °C/4h, 320 °C/4h, 350 °C/4h, 380 °C/4h.

The composites with 0%, 1%, 3%, 5% and 7% HNTs-c were labeled as PN, PN-HNTs-c1, PN-HNTs-c3, PN-HNTs-c5 and PN-HNTs-c7, respectively. At the same time, the composite materials with pure HNTs as filler were successively marked as PN, PN-HNTs-1, PN-HNTs-3, PN-HNTs-5 and PN-HNTs-7, respectively (see Table 1).

The prepared polymers were processed into appropriate size (40 mm × 10 mm × 2 mm) for Dynamic Mechanical Analysis (DMA) test, and the rest was used for Scanning Electron Microscope (SEM) observation section and Thermogravimetric Analyses (TGA).

2.6. Characterization methods

Fourier Transform Infrared (FTIR) spectra were recorded with a Bruker Vector 22 FTIR spectrometer. HNTs were mixed in KBr pellets and tested with wavenumbers between 4000 and 400 cm^{-1} in air. The Wide-angle X-ray Diffraction (WAXD) spectrum of HNTs and HNTs–phthalonitrile resin nanocomposites were taken by using a MiniFlex600 under the condition of 40 kV and 15 mA with Ni-filtered Cu Kα radiation ($\lambda = 0.15406$ nm) in reflection mode and

$$HNT(OH)+H_2O_3PPh \xrightarrow{Heat} HNT(HO_3PPh)+H_2O$$

Scheme 1. Chemical treatment of HNTs by phenylphosphonic acid (PPA).

the scanning speed was 4° min^{-1}. Thermogravimetric Analyses (TGA) were performed on a TA Instruments Q600 thermogravimetric analyzer from 25 to 1000 °C with nitrogen or air flow rate of 100 mL min^{-1}. Its heating rate was 10 °C min^{-1}. A TA Q800 dynamic mechanical analyzer was used to measure storage modulus (*E'*) and glass transition temperature (*Tg*) at a frequency of 1 Hz in single cantilever mode. The temperature range of the sample in the air was 30–380 °C and the heating rate was 5 °C min^{-1}. Scanning Electron Microscope (SEM; Nova Nano SEM450; FEI (Oregon State, USA)) operating at 10 kV was used to observe HNTs and the fracture surfaces morphology of polymers.

3. Results and discussion

3.1. Intercalation of HNTs with PPA

3.1.1. XRD characterization and analysis

Fig. 1 shows the respective XRD spectra of the as-received HNTs and the treated HNTs. For unmodified HNTs, we can find a sharp peak at $2\theta = 12.42°$, which corresponds to the internal (001) basal spacing of 7.12 Å. This is consistent with the previous report of Guo et al. [26]. However, a new sharp peak appeared near $2\theta = 5.9°$ after the treatment of halloysite nanotubes with PPA. This is due to the intercalation of PPA between interlayer positions, which expands the spacing of halloysite nanotubes layers [32,35]. The new sharp peaks of HNTs-a, HNTs-b, HNTs-c and HNTs-d are located at $2\theta = 5.98°$, 5.94°, 5.86°, and 5.88°, respectively, and their corresponding basal spacing are 14.77, 14.86, 15.08 and 15.01 Å. With the increase of PPA concentration, the layer distance of halloysite nanotubes increases gradually. However, the basal spacing of HNTs-c is larger than that of HNTs-d. This may be because when the weight ratio of PPA to HNTs is 2:1, the upper limit of the reaction has been reached. Even if the concentration of PPA increases, the layer distance of HNTs cannot be further extended because the hydroxyl groups that can react with halloysite have been transformed. Because the HNTs-c has the largest layer distance, which can make it fully contact with phthalonitrile resin, we choose HNTs-c as the fillers to prepare HNTs–phthalonitrile resin nanocomposites.

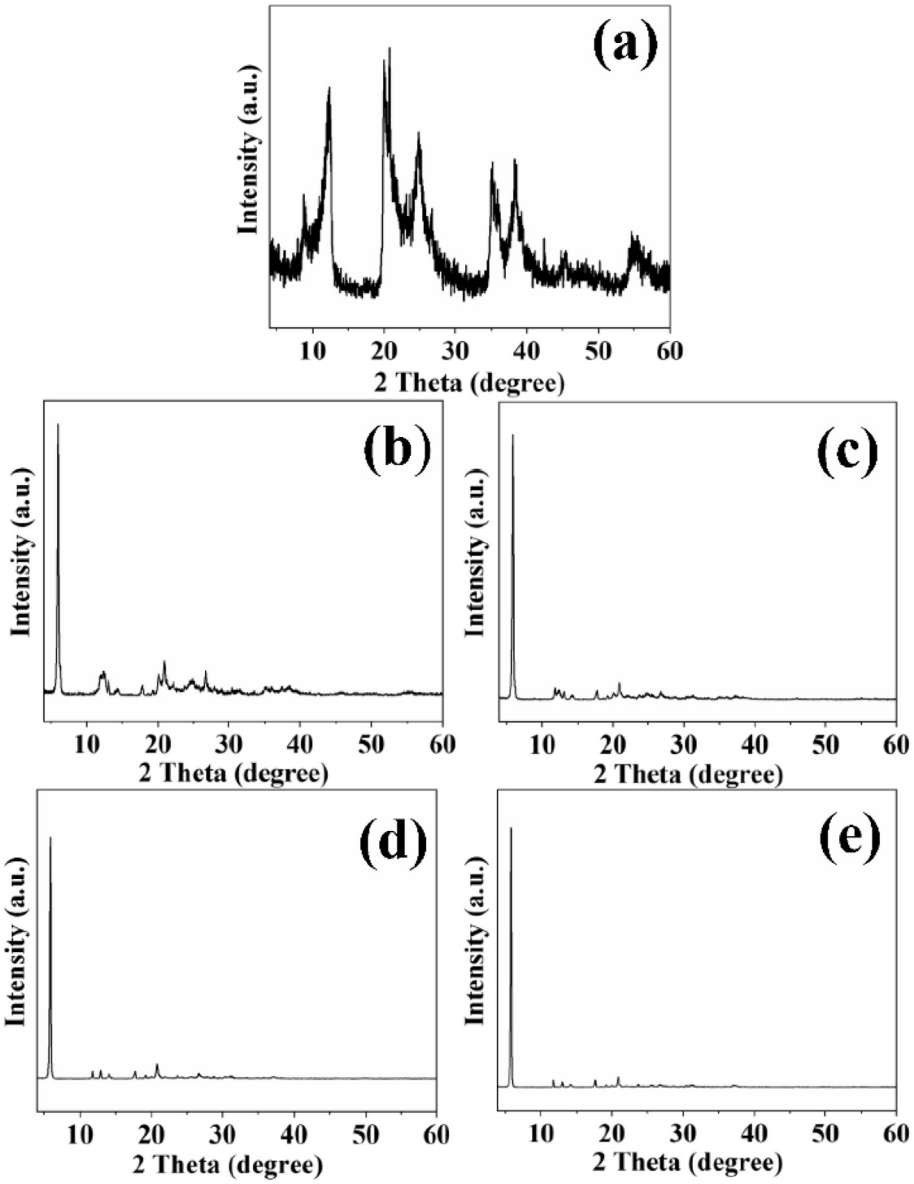

Fig. 1. WAXD patterns of (a) HNTs, (b) HNTs-a, (c) HNTs-b, (d) HNTs-c and (e) HNTs-d.

3.1.2. FTIR characterization and analysis

The infrared spectroscopy can show the change of halloysite nanotubes after intercalation more intuitively. Fig. 2 shows the infrared spectrum of HNTs after intercalation. Two absorption peaks at 750 and 692 cm^{-1} are attributed to the perpendicular Si—O stretching. Three characterization absorptions at 536, 468 and 432 cm^{-1} are on account of deformation of Al—O—Si, deformation of Si—O—Si and deformation of Si—O, respectively. Two characterization absorptions at 1089 and 1030 cm^{-1} can be ascribed to in-plane Si—O stretching. The absorption peaks at 1110 cm^{-1} belong to perpendicular Si—O stretching [35,38]. In the FTIR spectra of HNTs treated by PPA, new signals at 1168 cm^{-1} are observed, which are assigned to the P═O stretching peak [32]. Another new absorption peak at 1438 cm^{-1} is attributed to the stretching vibration of P—Ar. For spectra of HNTs-c and HNTs-d, the absorption peaks corresponding to the hydroxyl groups on halloysite nanotubes can not be found at 3698 and 3621 cm^{-1}. This confirms the existence of PPA on the halloysite nanotubes.

3.1.3. TGA characterization and analysis

The results of thermogravimetric analysis of the original and modified halloysite nanotubes are shown in Fig. 3. The rapid weight loss of samples at approximate 140 °C corresponds to the decomposition of crystal water in the halloysite nanotubes. After PPA intercalation, extra rapid weight loss of halloysite nanotubes occurs at about 620 °C, which may be caused by the decomposition of PPA when heated. The weight loss of pure halloysite nanotubes is 14.44% at 800 °C, while the mass loss of HNTs-a, HNTs-b, HNTs-c and HNTs-d are 25.82%, 31.89%, 36.65% and 38.21%, respectively. Therefore, the corresponding content of PPA in the inner layer or on the surface of halloysite nanotubes for samples of HNTs-a, HNTs-b, HNTs-c and HNTs-d are 11.38%, 17.45%, 22.21% and 23.77%.

3.1.4. SEM characterization and analysis

Fig. 4 exhibits the SEM micrographs of pure HNTs, HNTs-a, HNTs-b, HNTs-c and HNTs-d, respectively. As shown in Fig. 4a, the longer HNTs tend to be intertwined with each other to form agglomerates that cannot be evenly dispersed in the polymer. In fact, HNTs are rolled tubes composed of many tightly arranged

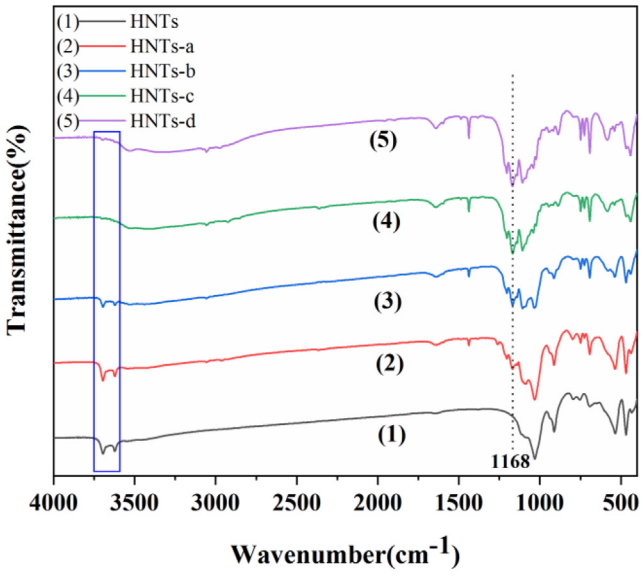

Fig. 2. FTIR spectra of pure HNTs and HNTs treated by PPA.

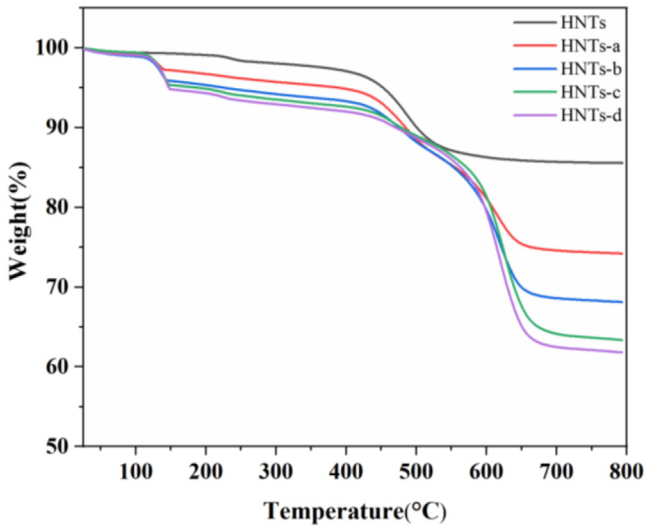

Fig. 3. TGA curves of pure HNTs and HNTs treated by PPA.

aluminosilicate sheets. However, as shown in Fig. 4b-e, after the modification of halloysite nanotubes by PPA, the interlayer spacing of HNTs expanded with the shedding of a lot of halloysite sheets. With the increase of PPA concentration, the peeling off sheets of halloysite gradually increased. These sheets are independent of each other, which is more conducive to their uniform distribution in polymers. And it is very beneficial to improve the performance of polymers .

3.2. Characterizations of the HNTs—phthalonitrile resin nanocomposites

3.2.1. Dynamic mechanical analysis

The Dynamic Mechanical Analysis (DMA) test was used to study the thermomechanical properties of the HNTs—phthalonitrile resin nanocomposites. And it is a sensitive method to determine the glass transition temperature *(Tg)* of polymers [27]. Fig. 5a shows the storage modulus (E') of the pure resin and resin/HNTs nanocomposites with pure HNTs as fillers in the range of 30—380 °C. When HNTs were not added, the storage modulus of the polymer at 30 °C and 380 °C are 2670 and 1542 MPa, respectively. This shows that the polymer itself has excellent thermomechanical properties. With the continuous increase of HNTs content, the storage modulus of polymers shows an upward trend. When the pure HNTs content is 7%, the storage modulus of polymers at 30 °C and 380 °C is as high as 2963 and 1753 MPa, respectively. Compared with that of the polymer without fillers, the storage modulus of the resin/HNTs nanocomposite increases by 10.97% and 13.68%, respectively. Fig. 5b reveals the storage modulus (E') of the pure resin and resin/HNTs-c nanocomposites with HNTs-c as fillers in the range of 30—380 °C. When the HNTs-c content is 7%, the corresponding storage modulus of polymers at 30 °C and 380 °C is 3111 and 1780 MPa, which increased by 16.52% and 15.43%, respectively, in comparison with the polymer without fillers. This shows that HNTs as the filler can significantly improve the thermomechanical properties of polymers. Because the modified HNTs have a better dispersion in the polymers, the use of HNTs-c as the filler has a more active role in improving the thermomechanical properties of the polymers. At the same time, the loss tangent (tan δ) of the pure resin, resin/HNTs nanocomposites and resin/HNTs-c nanocomposites are shown in Fig. 6. The peak value of tan δ indicates the *Tg* of polymers. We can find that the tan δ curve of HNTs—phthalonitrile resin

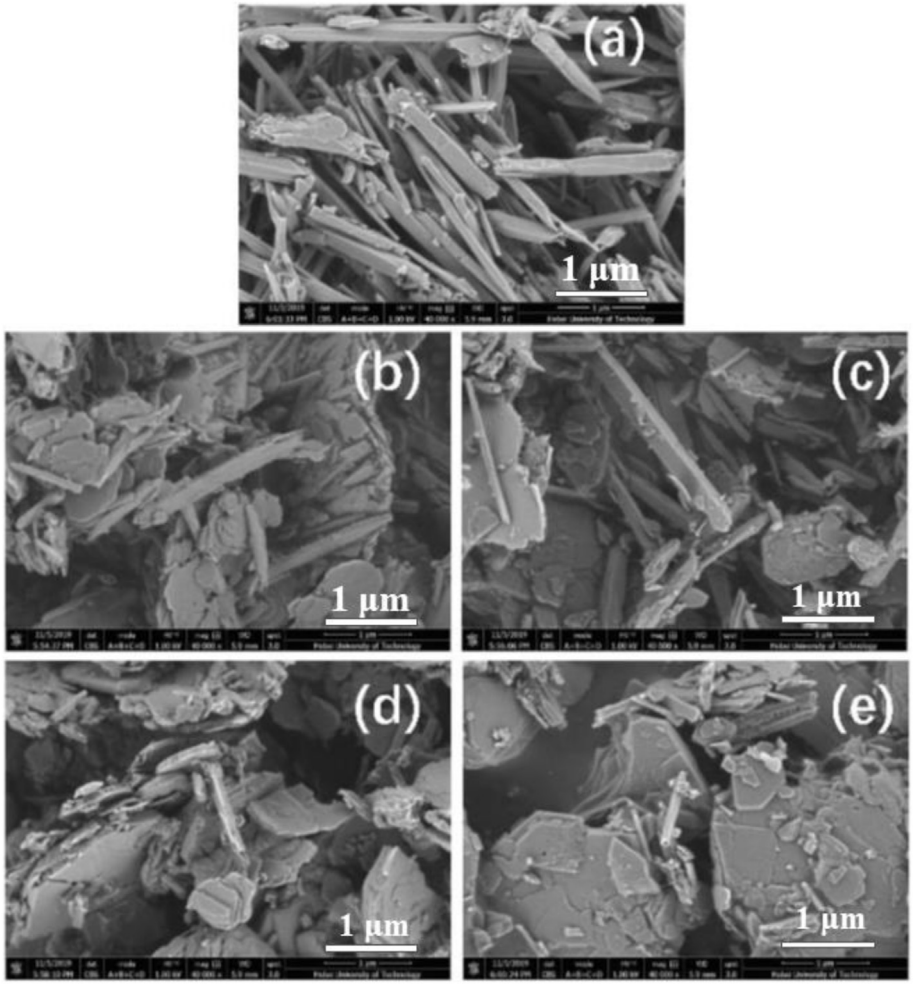

Fig. 4. SEM micrographs of (a) HNTs, (b) HNTs-a, (c) HNTs-b, (d) HNTs-c and (e) HNTs-d.

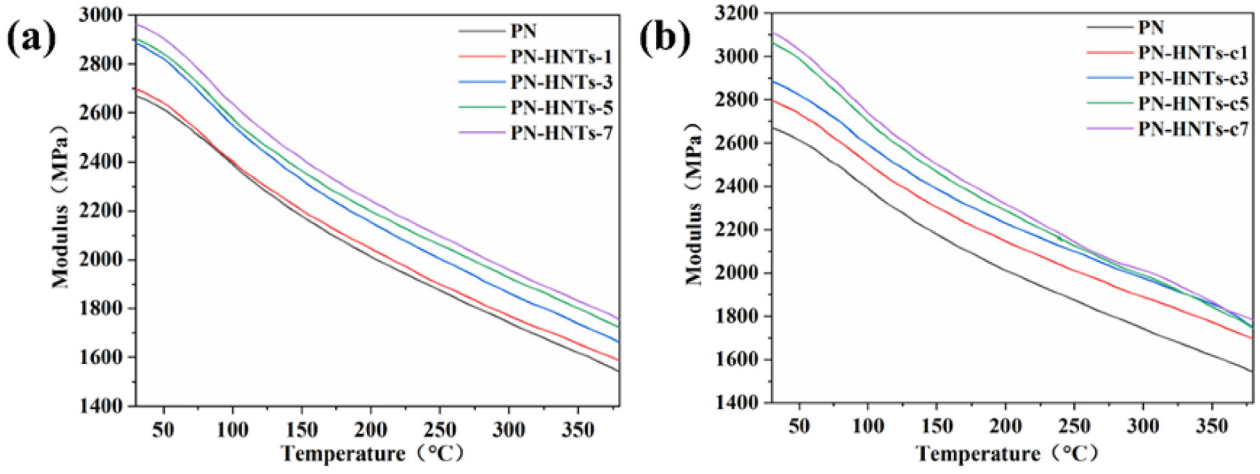

Fig. 5. Evolution of E′ of (a) resin/HNTs nanocomposites and (b) resin/HNTs-c nanocomposites.

nanocomposites have no obvious peak value in the range of 30–380 °C, which indicates that the glass transition temperature of polymers are higher than 380 °C and its upper temperature limit is greater than 380 °C. The thermomechanical properties of all polymers are collected in Table 2.

3.2.2. Thermal and thermal-oxidative stabilities

TGA can be used to quantitatively measure material quality changes related to transformation and thermal degradation [27]. Fig. 7a shows the TGA curves of pure resin and resin/HNTs-c nanocomposites in inert atmosphere, with Fig. 7b representing

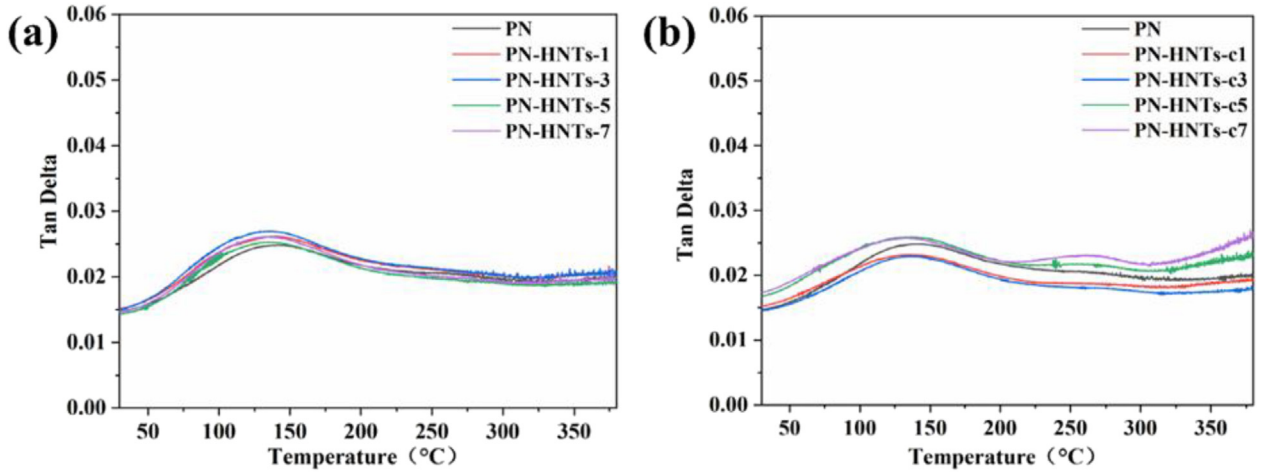

Fig. 6. Evolution of tan δ of (a) resin/HNTs nanocomposites and (b) resin/HNTs-c nanocomposites.

Table 1
Type and content of fillers in nanocomposites.

Samples name	Filler type	Filler content (wt.%)
PN	–	0
PN-HNTs-c1	HNTs-c	1
PN-HNTs-c3	HNTs-c	3
PN-HNTs-c5	HNTs-c	5
PN-HNTs-c7	HNTs-c	7
PN-HNTs-1	HNTs	1
PN-HNTs-3	HNTs	3
PN-HNTs-5	HNTs	5
PN-HNTs-7	HNTs	7

those of resin/HNTs nanocomposites. Fig. 7c and d exhibit the weight loss curve of the pure resin, resin/HNTs-c nanocomposites and resin/HNTs nanocomposites in air atmosphere at 25–1000 °C. We can find that the unfilled resin has excellent thermal stability. Under nitrogen atmosphere, the temperatures of 5% and 10% weight loss of the unfilled resin are 510 and 547 °C, respectively. In an air atmosphere, the corresponding temperatures of 5% and 10% weight loss are 513 and 551 °C. Therefore, their thermal and thermal-oxidative stabilities are better than those of many other previously reported phthalonitrile resin. When the content of HNTs-c is 1%, the polymer has the best thermal stability. The temperature of 5% weight loss in nitrogen and air are 516 and 519 °C, respectively. The structure of phthalonitrile resin is a highly crosslinked network structure, which mainly exists in three forms: polyindoline, polytriazine and phthalocyanine [37]. When a molecular chain breaks, only a part of the polymer breaks, but it still remains connected with the main body of the polymer. On the other hand, the structure of phthalonitrile resin is composed of aromatic ring skeleton, which is the important basis of high temperature resistance of polymer. The bond energy of the chemical bond that makes up the molecular structure of materials and the density of H atom usually affect the thermal stability of materials. The resin matrix used in this experiment includes C–C bond (348 kJ mol^{-1}), C–O bond (360 kJ mol^{-1}), C=N bond (613 kJ mol^{-1}) and C=C bond (518 kJ mol^{-1}) [39]. When the material is in high temperature environment, the structure of alkyl chain segment, benzene ring and aromatic heterocycle containing N atom will decompose in turn. Therefore, more stable structures can be introduced into phthalonitrile via molecular design to obtain phthalonitrile resin with high thermal stability. When HNTs-c are added, the heat capacity of halloysite is large, so it can absorb heat well. It was evenly dispersed in the resin matrix, which can prevent the volatilization of small molecular oxides in the process of thermal decomposition, so that the composite began to decompose at a higher temperature. However, with the increase of fillers, the thermal stability of the polymer began to deteriorate. At this time, the delay of the decomposition of polymer by the halloysite nanotube has a competitive relationship with the decomposition of PPA on the HNTs. This may be due to the easy decomposition of PPA on the halloysite nanotube at high temperature. When pure HNTs are selected as the filler, the thermal stability of the polymers increases as the filler content increases. This is mainly because the HNTs have better thermal stability and prevent the evaporation of small molecules generated during heating.

Table 2
Storage modulus and glass transition temperature of pure resin and composites.

Samples	Storage Modulus		*Tg* (°C)
	30 °C (MPa)	380 °C (MPa)	
PN	2670	1542	>380 °C
PN-HNTs-c1	2795	1696	>380 °C
PN-HNTs-c3	2883	1747	>380 °C
PN-HNTs-c5	3064	1744	>380 °C
PN-HNTs-c7	3111	1781	>380 °C
PN-HNTs-1	2697	1586	>380 °C
PN-HNTs-3	2885	1661	>380 °C
PN-HNTs-5	2890	1723	>380 °C
PN-HNTs-7	2963	1753	>380 °C

For halogen-free polymers, according to Van Krevelen equation [40], the limit oxygen index (LOI) and carbon residue rate (CR_2) of the materials conform to the following relationship. As shown in equation (1):

$$LOI = 17.5 + 0.4(CR_2) \quad (1)$$

LOI is the volume fraction of oxygen in the mixture of oxygen and nitrogen when the polymer is just able to support its combustion. CR_2 is the carbon residue rate of the material at 850 °C in nitrogen. The calculated LOI value of pure resin is 47.8. When HNTs were added as a filler, the LOI value of the polymer has been improved to varying degrees. Among them, the maximum LOI value of PN-HNTs-7 is 48.7. When the LOI value is greater than 26, the material can be regarded as a flame retardant material [5]. Therefore, the prepared nanocomposite is a material with excellent flame

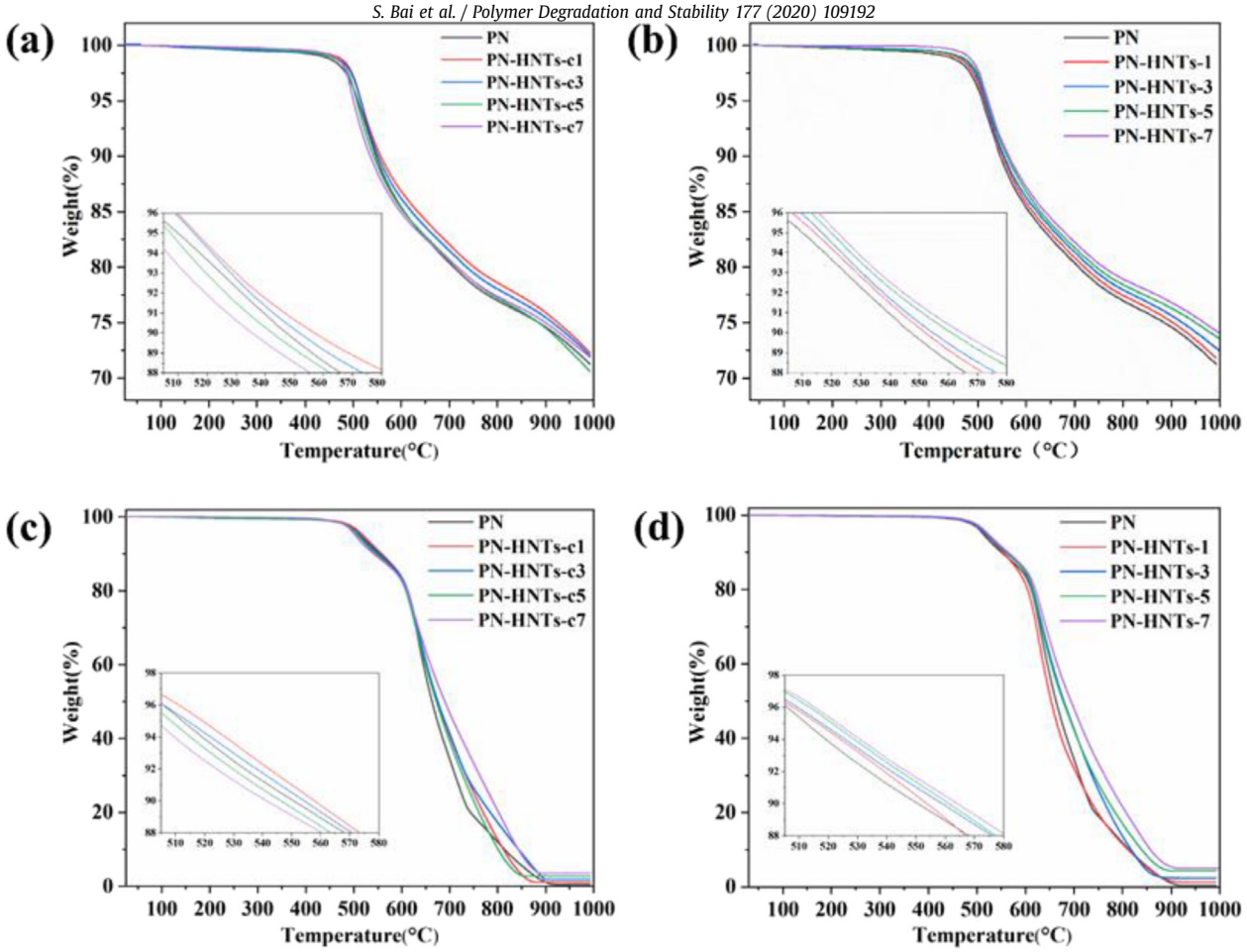

Fig. 7. TGA curves of (a) resin/HNTs-c nanocomposites and (b) resin/HNTs nanocomposites in inert atmosphere; (c) resin/HNTs-c nanocomposites and (d) resin/HNTs in air atmosphere.

retardancy.

Characteristic temperatures of thermal and thermal oxidation stability of the polymers are summarized in Table 3.

3.2.3. XRD characterization and analysis

The Wide-angle X-ray Diffraction (WAXD) is used to reveal the intercalation of HNTs in the nanocomposite. Fig. 8 shows the XRD patterns of the pure resin and the nanocomposites. We can see that the unfilled phthalonitrile resin shows a wide and slow hump, which indicates that the polymer is an amorphous material. When HNTs-c are added to polymers, a sharp peak appears around $2\theta = 6.1$, which corresponds to the modified halloysite nanotubes. And with the increase of the filler, the sharp peak becomes more obvious. When pure HNTs were added as filler, the characteristic peaks of pure HNTs were also found around 2θ = 12 and 24,

Table 3
Thermal parameters of pure resin and composites in inert and air atmosphere.

	In nitrogen			In air			LOI
	$T_{5\%}$/°C	$T_{10\%}$/°C	CR/%	$T_{5\%}$/°C	$T_{10\%}$/°C	CR/%	
PN	510	547	71	513	551	–	47.8
PN-HNTs-c1	516	557	72	519	558	1	48.4
PN-HNTs-c3	515	552	72	514	554	2	48.2
PN-HNTs-c5	507	542	71	509	546	3	48.0
PN-HNTs-c7	501	536	72	503	541	4	48.0
PN-HNTs-1	514	552	72	516	554	1	48.0
PN-HNTs-3	517	555	73	518	559	2	48.3
PN-HNTs-5	520	561	74	521	561	4	48.5
PN-HNTs-7	522	565	74	523	564	5	48.7

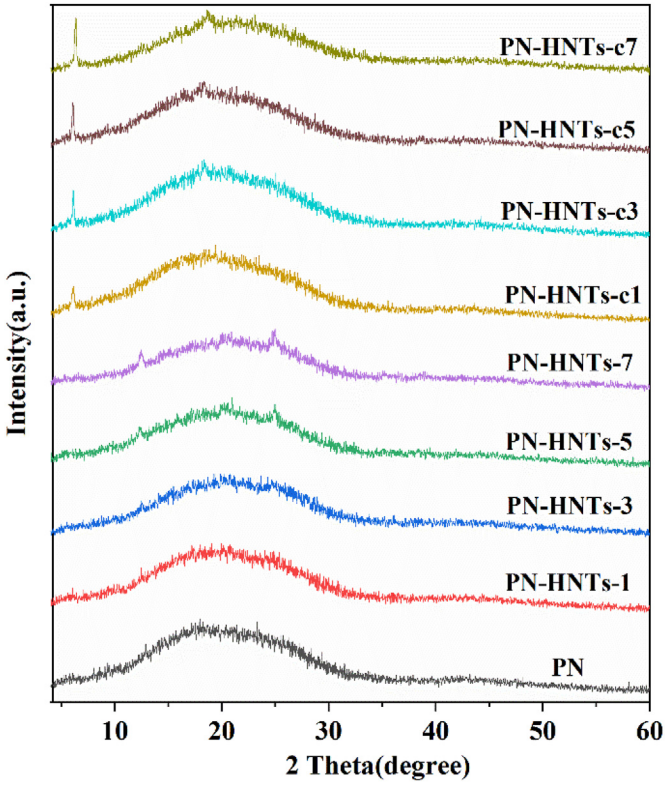

Fig. 8. WAXD patterns of pure resin and the nanocomposites.

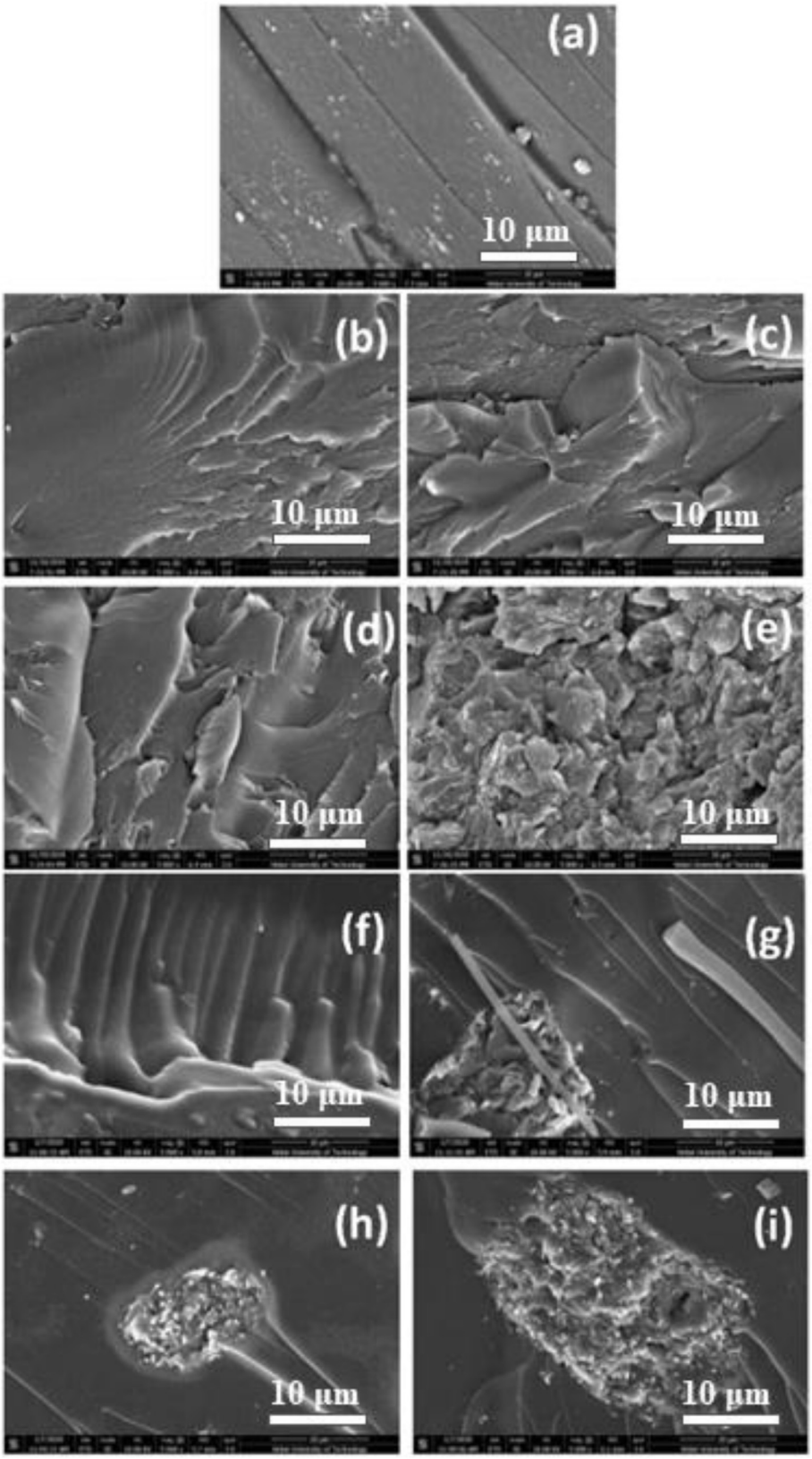

Fig. 9. SEM micrographs of fracture surface of (a) pure resin, (b) PN-HNTs-c1, (c) PN-HNTs-c3, (d) PN-HNTs-c5, (e)PN-HNTs-c7, (f) PN-HNTs-1, (g) PN-HNTs-3, (h) PN-HNTs-5 and (i) PN-HNTs-7.

respectively. This indicates that the intercalation structure of halloysite nanotubes is still retained in polymers.

3.2.4. SEM characterization and analysis

Scanning electron microscopy (SEM) is used to observe and analyze the cross-section of polymers. Fig. 9 presents the SEM micrographs of fracture surfaces of the pure resin and the nanocomposites. In Fig. 9a for the pure resin, it is seen that the crack growth of phthalonitrile resin without fillers shows the same obvious distribution as that of rivers, and all cracks are almost parallel, which is the feature of brittle fracture. It shows that when the polymer is under stress, the initial crack propagates in a uniform environment without any obstacles, resulting in long fracture line and poor strength. When HNTs-c were added as the filler, with the increase of fillers, these particles hinder the propagation of force. When the force is transferred to halloysites, it will deviate to another direction to cushion the stress. With the increase of fillers, the deviation is more frequent and the size of cracks is gradually reduced, so the energy requires to destroy the composite material gradually increases. With the increase of the filler, the crack size of the fracture gradually decreases, and the cross-section morphology becomes rougher. However, when pure HNTs were used as the filler, HNTs will agglomerate obviously in the polymers due to their entangled structure, which also proves that the improvement of thermal mechanical properties of HNTS-c are more beneficial. The results are consistent with the observed morphology.

4. Conclusions

Phenylphosphonic acid (PPA) was successfully used to modify halloysite nanotubes (HNTs). The structure of HNTs after modification were analyzed by Wide-angle X-ray Diffraction (WAXD), Fourier Transform Infrared spectroscopy (FTIR), Thermogravimetric Analysis (TGA) and Scanning Electron Microscope (SEM). The WAXD results showed that when the weight ratio of PPA to HNTs was 2:1, the basal spacing of HNTs expended from 7.12 Å to 15.08 Å. PPA residence on the halloysite nanotubes was further proved by FTIR and TGA. The effect of PPA concentration on HNTs were observed by SEM, which implies that with the increase of PPA concentration, the peeling off sheets of halloysite gradually increased. These sheets avoid the entanglement of halloysite nanotubes. When the HNTs-c content is 7%, the storage modulus of polymers at 30 °C and 380 °C is as high as 3111 and 1780 MPa, respectively. When pure HNTs were used as the fillers, the thermal stability and thermal oxidation stability of the polymer increased with the increase of the fillers. The limit oxygen index (LOI) of nanocomposites also increased. However, when HNTs-c were used as the fillers, the thermal stability and thermal oxidation stability of the polymers increased first and then decreased with the increase of the fillers. This may be due to the competitive relationship between the stability of halloysite nanotubes to polymers and the thermal decomposition of the PPA in high temperature environment. WAXD analysis of the polymers shows that the corresponding structures of HNTs are preserved in the polymers. It was found by SEM that HNTs-c dispersed well and pure HNTs agglomerated in the polymers. The uniform distribution of HNTs-c in the matrix is the key factor for the composite to have more excellent thermal properties. It can absorb part of the heat and hinder the volatilization of small molecular products. Because of the better dispersion of HNTs treated by PPA in the polymers, the polymers with HNTs-c as fillers have more excellent thermomechanical properties than the polymers with pure HNTs as fillers. Since the prepared composites have excellent thermomechanical properties, thermal stability and thermal oxidation stability, they are expected to have wide application prospects in fields of aerospace, engine shell, electronic package and the like. At the same time, fillers with special properties should also be sought to meet the needs of social development for materials.

Declaration of competing interest

The authors declare that they have no known competing financial interests or personal relationships that could have appeared to influence the work reported in this paper.

CRediT authorship contribution statement

Shengnan Bai: Conceptualization, Formal analysis, Writing - original draft. **Xinyu Sun:** Investigation, Writing - review & editing. **Minjie Wu:** Validation. **Xiaoyu Shi:** Visualization. **Xinggang Chen:** Data curation. **Xiaoyan Yu:** Project administration, Funding acquisition. **Qingxin Zhang:** Resources, Supervision, Funding acquisition.

Acknowledgements

The author would like to gratefully acknowledge the financial support from the National Natural Science Foundation of China (51573037), Natural Science Foundation of Hebei Province, China (B2017202281, E2019202348) and Youth Natural Science Foundation of Hebei Province, China (E2019209514).

References

[1] T.M. Keller, D.D. Dominguez, High temperature resorcinol-based phthalonitrile polymer, Polymer 46 (2005) 4614–4618.
[2] M. Laskoski, D.D. Dominguez, T.M. Keller, Alkyne-containing phthalonitrile resins: controlling mechanical properties by selective curing, J. Polym. Sci., Part A: Polym. Chem. 51 (2013) 4774–4778.
[3] S. Ji, P. Yuan, J. Hu, R. Sun, K. Zeng, G. Yang, A novel curing agent for phthalonitrile monomers: curing behaviors and properties of the polymer network, Polymer 84 (2016) 365–370.
[4] M. Laskoski, A. Neal, M.B. Schear, T.M. Keller, H.L. Ricks-Laskoski, A.P. Saab, Oligomeric aliphatic–aromatic ether containing phthalonitrile resins, J. Polym. Sci., Part A: Polym. Chem. 53 (2015) 2186–2191.
[5] H. Wang, J. Wang, H. Guo, X. Chen, X. Yu, Y. Ma, P. Ji, K. Naito, Z. Zhang, Q. Zhang, A novel high temperature vinylpyridine-based phthalonitrile polymer with a low melting point and good mechanical properties, Polym. Chem. 9 (2018) 976–983.
[6] P. Yuan, S. Ji, J. Hu, X. Hu, K. Zeng, G. Yang, Systematic study on highly efficient thermal synergistic polymerization effect between alicyclic imide moiety and phthalonitrile: scope, properties and mechanism, Polymer 102 (2016) 266–280.
[7] M. Laskoski, D.D. Dominguez, T.M. Keller, Synthesis and properties of a bisphenol A based phthalonitrile resin, J. Polym. Sci., Part A: Polym. Chem. 43 (2005) 4136–4143.
[8] M. Derradji, X. Song, A.Q. Dayo, J. Wang, W.-b. Liu, Highly filled boron nitride-phthalonitrile nanocomposites for exigent thermally conductive applications, Appl. Therm. Eng. 115 (2017) 630–636.
[9] A. Gallego, B. Herrera, R. Buitrago-Sierra, C. Zapata, K. Cacua, Influence of filling ratio on the thermal performance and efficiency of a thermosyphon operating with Al_2O_3-water based nanofluids, Nano-Struct. Nano-Objects 22 (2020), https://doi.org/10.1016/j.nanoso.2020.100448.
[10] Y.M. Alrababah, C.K. Sheng, M.F. Hassan, Influence of ammonium nitrate concentration on structural evolution and optical properties tuning of CdS nanoparticles synthesized by precipitation method, Nano-Struct. Nano-Objects 19 (2019), https://doi.org/10.1016/j.nanoso.2019.100344.
[11] J. Joy, C. Jose, X.Y. Yu, L. Mathew, S. Thomas, S. Pilla, The influence of nanocellulosic fiber, extracted from Helicteres isora, on thermal, wetting and viscoelastic properties of poly(butylene succinate) composites, Cellulose 24 (2017) 4313–4323.
[12] K.A. Krishnan, C. Jose, K.R. Rohith, K.E. George, Sisal nanofibril reinforced polypropylene/polystyrene blends: morphology, mechanical, dynamic mechanical and water transmission studies, Ind. Crop. Prod. 71 (2015) 173–184.
[13] M. Okada, A. Takeyama, Y. Yamada, Thermal hysteresis control of VO_2 (M) nanoparticles by Ti-F cooping, Nano-Struct. Nano-Objects 20 (2019), https://doi.org/10.1016/j.nanoso.2019.100395.
[14] B.D.S. Deeraj, R. Harikrishnan, J.S. Jayan, A. Saritha, K. Joseph, Enhanced viscoelastic and rheological behavior of epoxy composites reinforced with polyimide nanofiber, Nano-Struct. Nano-Objects 21 (2020), https://doi.org/10.1016/j.nanoso.2019.100421.

[15] K. Sahu, S. Choudhary, S.A. Khan, A. Pandey, S. Mohapatra, Thermal evolution of morphological, structural, optical and photocatalytic properties of CuO thin films, Nano-Struct. Nano-Objects 17 (2019) 92–102.
[16] S. Shan, X. Chen, Z. Xi, X. Yu, X. Qu, Q. Zhang, The effect of nitrile-functionalized nano-aluminum oxide on the thermomechanical properties and toughness of phthalonitrile resin, High Perform. Polym. 29 (2017) 113–123.
[17] M. Derradji, N. Ramdani, L.d. Gong, J. Wang, X.d. Xu, Z.w. Lin, A. Henniche, W.b. Liu, Mechanical, thermal, and UV-shielding behavior of silane surface modified ZnO-reinforced phthalonitrile nanocomposites, Polym. Adv. Technol. 27 (2016) 882–888.
[18] M. Derradji, N. Ramdani, T. Zhang, J. Wang, L.-d. Gong, X.-d. Xu, Z.-w. Lin, A. Henniche, H. Rahoma, W.-b. Liu, Effect of silane surface modified titania nanoparticles on the thermal, mechanical, and corrosion protective properties of a bisphenol-A based phthalonitrile resin, Prog. Org. Coating 90 (2016) 34–43.
[19] M. Derradji, N. Ramdani, T. Zhang, J. Wang, Z.-w. Lin, M. Yang, X.-d. Xu, W.-b. Liu, High thermal and thermomechanical properties obtained by reinforcing a bisphenol-A based phthalonitrile resin with silicon nitride nanoparticles, Mater. Lett. 149 (2015) 81–84.
[20] X. Yang, Y. Zhan, J. Yang, H. Tang, F. Meng, J. Zhong, R. Zhao, X. Liu, Effect of nitrile functionalized graphene on the properties of poly (arylene ether nitrile) nanocomposites, Polym. Int. 61 (2012) 880–887.
[21] U.A. Handge, K. Hedicke-Höchstötter, V. Altstädt, Composites of polyamide 6 and silicate nanotubes of the mineral halloysite: influence of molecular weight on thermal, mechanical and rheological properties, Polymer 51 (2010) 2690–2699.
[22] A. Alhuthali, I.M. Low, Water absorption, mechanical, and thermal properties of halloysite nanotube reinforced vinyl-ester nanocomposites, J. Mater. Sci. 48 (2013) 4260–4273.
[23] H. Ismail, S. Salleh, Z. Ahmad, Properties of halloysite nanotubes-filled natural rubber prepared using different mixing methods, Mater. Eng. 50 (2013) 790–797.
[24] V. Khunova, J. Kristóf, I. Kelnar, J. Dybal, The effect of halloysite modification combined with in situ matrix modifications on the structure and properties of polypropylene/halloysite nanocomposites, Express Polym. Lett. 7 (2013).
[25] E. Abdullayev, A. Joshi, W. Wei, Y. Zhao, Y. Lvov, Enlargement of halloysite clay nanotube lumen by selective etching of aluminum oxide, ACS Nano 6 (2012) 7216–7226.
[26] M. Du, B. Guo, D. Jia, Thermal stability and flame retardant effects of halloysite nanotubes on poly (propylene), Eur. Polym. J. 42 (2006) 1362–1369.
[27] J. James, K.P. Pramoda, S. Thomas, Polymers and Multicomponent Polymeric Systems Thermal, Thermo-Mechanical and Dielectric Analysis, CRC Press, Boca Raton, 2019, https://doi.org/10.1201/9780429486609.
[28] J. James, G.V. Thomas, P.K. Pallathadka, N. Kalarikkal, S. Thomas, Thermoplastic-Elastomer composition based on Interpenetrating Polymeric Network of styrene butadiene Rubber- Poly (Methyl methacrylate) as efficient vibrational damper, New J. Chem. 42 (2018) 1939–1951.
[29] D.D. Wu, N. Sinha, J. Lee, B.P. Sutherland, N.I. Halaszynski, Y. Tian, J. Caplan, H.V. Zhang, J.G. Saven, C.J. Kloxin, D.J. Pochan, Polymers with controlled assembly and rigidity made with click-functional peptide bundles, Nature 574 (2019) 658–662.
[30] N.J. Sinha, D.D. Wu, C.J. Kloxin, J.G. Saven, G.V. Jensen, D.J. Pochan, Polyelectrolyte character of rigid rod peptide bundlemer chains constructed via hierarchical self-assembly, Soft Matter 15 (2019) 9858–9870.
[31] K.S. Lee, Y.W. Chang, Thermal, mechanical, and rheological properties of poly (ε-caprolactone)/halloysite nanotube nanocomposites, J. Appl. Polym. Sci. 128 (2013) 2807–2816.
[32] Y. Tang, S. Deng, L. Ye, C. Yang, Q. Yuan, J. Zhang, C. Zhao, Effects of unfolded and intercalated halloysites on mechanical properties of halloysite–epoxy nanocomposites, Composites, Part A 42 (2011) 345–354.
[33] P.P. Vijayan, Y.M.H. El-Gawady, M. Al-Maadeed, A comparative study on long term stability of self-healing epoxy coating with different inorganic nanotubes as healing agent reservoirs, Express Polym. Lett. 11 (2017) 863–872.
[34] S. Sharma, A.A. Singh, A. Majumdar, B.S. Butola, Tailoring the mechanical and thermal properties of polylactic acid-based bionanocomposite films using halloysite nanotubes and polyethylene glycol by solvent casting process, J. Mater. Sci. 54 (2019) 8971–8983.
[35] J.L. Guimarães, P. Peralta-Zamora, F. Wypych, Covalent grafting of phenylphosphonate groups onto the interlamellar aluminol surface of kaolinite, J. Colloid Interface Sci. 206 (1998) 281–287.
[36] M.E. Boyle, J.D. Adkins, A.W. Snow, R.F. Cozzens, R.F. Brady Jr., Synthesis and characterization of melt-polymerizable aminophthalocyanine monomers, J. Appl. Polym. Sci. 57 (1995) 77–85.
[37] S. Bai, X. Sun, Z. Zhang, X. Chen, X. Yu, Q. Zhang, Synthesis and properties of A low melting point phthalonitrile resin containing high density nitrile groups, ChemistrySelect 5 (2020) 265–269.
[38] P. Yuan, P.D. Southon, Z. Liu, M.E. Green, J.M. Hook, S.J. Antill, C.J. Kepert, Functionalization of halloysite clay nanotubes by grafting with γ-aminopropyltriethoxysilane, J. Phys. Chem. C 112 (2008) 15742–15751.
[39] H. Sheng, X. Peng, H. Guo, X. Yu, C. Tang, X. Qu, Q. Zhang, Synthesis and thermal properties of a novel high temperature alkyl-center-trisphenolic-based phthalonitrile polymer, Mater. Chem. Phys. 142 (2013) 740–747.
[40] D. Van Krevelen, Some basic aspects of flame resistance of polymeric materials, Polymer 16 (1975) 615–620.